

Feasibility of Communication Between Sensor Nodes On-board Spacecraft Using Multi Layer Insulation

Saba Akbari¹, Jan Bergman², Thiemo Voigt¹, Jesper Fredriksson², Klas Hjort³

¹Uppsala University, Department of Electrical Engineering, ²Swedish Institute of Space Physics,

³Uppsala University, Department of Material Science and Engineering

{saba.akbari; thiemo.voigt; klas.hjort@angstrom.uu.se} {jb; jesper.fredriksson@irfu.se}

Abstract

Cables and connectors constitute a large portion of a spacecraft payload, 5% and more. Therefore, a reduction in the number of cables decreases the launch costs and increases the payload portion of spacecrafts. In spacecrafts, wireless links have reliability issues and hence other solutions are needed. Multi-layer insulation (MLI) is used to minimize heat loss from the spacecraft to the outer space and also to protect the spacecraft components from overheating, during sun illumination. An MLI structure contains conductive layers with spacers between them which should make it possible to use the MLI for communication, similar to power-line communications. By assigning one layer as power and the other one as ground, it should be possible to both transfer data and power over the MLI. In this paper we develop a schematic solution for power and data transfer over MLI. We demonstrate experimental results that show the feasibility of this concept.

Categories and Subject Descriptors

Hardware [Communication hardware, interfaces and storage]: Sensor applications and deployments

General Terms

Design, Communication, Experimentation

Keywords

Multi-layer insulation, in-spacecraft communication, embedded sensing, power-line communications (PLC)

1 Introduction

The increasing applications of sensor networks have become more tangible in our daily lives. Sensor networks are used in different fields such as environmental monitoring [2], structural health monitoring [13], and biomedicine [4]. In spacecrafts, there are embedded sensor nodes to, for example, measure temperature [9] and to detect impacts from mi-

cro-meteorites [8]. Micrometeorites and artificial debris are one of the components of the space medium in low earth orbits. Micrometeorites have an average velocity of 20 km/s. Artificial debris, e.g., satellite breakups have an average velocity of 8.7 km/s [5]. Therefore, micrometeorites and artificial debris can bring damage to spacecrafts [7]. In order to analyze the behavior of a micrometeorite cloud, a spacecraft can be equipped with sensors for micrometeorite detection [7]. Connecting sensors via cables, however, adds additional weight to a spacecraft. For example, in small satellites cables account for 5-10% of the total weight and this percentage increases for larger satellites [10]. A reduction in the number of cables will decrease the launch costs and allow for additional payload. Connecting sensors via low-power wireless technologies such as Bluetooth or ZigBee would also be attractive but there are doubts regarding the reliability of the wireless links in spacecrafts [10].

Spacecrafts use heat insulation layers, so-called multi-layer insulation (MLI), to minimize heat transfer from the spacecraft surface to the space. Due to its structure, the MLI prevents excessive heating and cooling of the surroundings. The former could be caused from a spacecraft internal components with excessive heat dissipation. MLI blankets are deployed over the exterior parts of the spacecraft [3]. Fig. 1 demonstrates the structure of an MLI. As shown in Fig. 1, an MLI consists of conductive layers with netting spacers placed between each conductive layer. Therefore, the MLI could be used as a communication and power transfer medium by assigning one layer as power and the other one as ground, similar to power-line communications (PLC) [14].

In this paper, we therefore propose to use the spacecraft MLI to network and power sensors. Towards this end, the paper makes the following contributions:

- We motivate why the MLI can be considered as a medium for communication in spacecrafts.
- We develop a schematic solution for communication and power transfer over the MLI.
- We carry out experiments based on the developed schematic solution that investigate the feasibility of communication between sensor nodes through MLI. We demonstrate communication and power transfer over the MLI without disturbing its primary functionality.

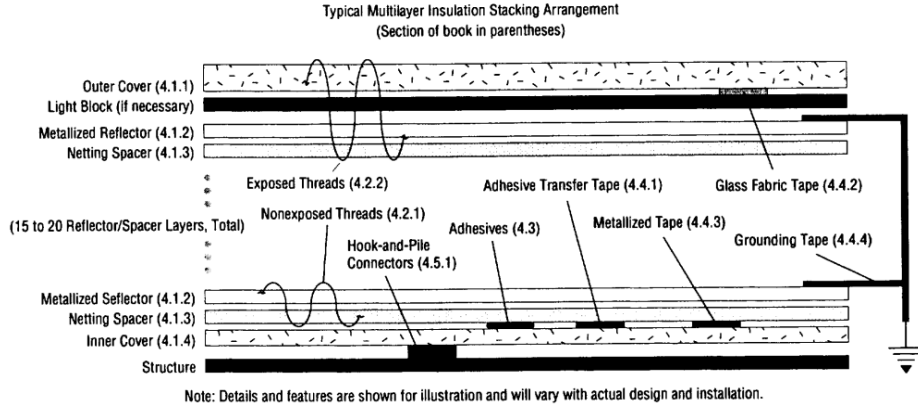


Figure 1. Cross section of an MLI blanket [6]

The rest of the paper is structured as follows: Section 2 provides an overview of the related work. Section 3 provides theoretical and experimental rationales of why we consider MLI as a medium for communication. Section 4 presents our MLI-based communication platform. Section 5 illustrates the experiment we perform to evaluate communication between sensor nodes through MLI and finally Section 6 provides conclusive remarks.

2 Related Work

PLC has been used in different industrial sectors. Zhilenkov et al. analyzed the possibility of using PLC in automation industry and more specifically a drilling rig [18]. The authors provide two reasons for using PLC: First, the drilling rig can be represented as a metallic construction which could lead to the attenuation of WiFi signals. Also, interference caused by the rig drive complicates the use of WiFi. Second, the large number of cables used on the rig site can be replaced by PLC. TextileNet was one of the first works using PLC for fabrics [16]. It uses two conductive fabric layers: one for power and the other as ground. TextileNet employs a DC approach according to which either charging or communication takes place at a time. It uses baseband communication and achieves a bitrate of 10 kb/s [16]. In order to apply TextileNet to real life, it is necessary to make sure that capacitor charging is fast enough to provide energy for the periods when communication takes place. Shinoda et al. study the impedance characteristics of garment [17]. For instance, they have shown that if they represent a garment as cylindrical sections, the resistance vs distance graph can have a linear or logarithmic behavior depending on the diameter of the fabric.

Using three layers of fabric for power line communication, i.e., the first layer for power, second as ground and the third one as the insulator between the first two layers could result in thicker fabrics [11]. Noda and Shinoda propose a PLC architecture that uses one fabric layer as an insulating layer and conductive threads sewn (i.e., power and ground layers) on both sides of the fabric. Moreover, the same work uses frequency division multiplexing (FDM) which enables on-off control of the receivers using different frequencies. This approach does not switch on/off the DC power

and therefore, the power supply is provided continuously to the sensor nodes. The FDM approach is used in their later work [12] for sensors with I2C interface where clock and data signals are transmitted separately. In contrast, our communication platform does not operate with I2C and we transmit a self-clocked signal. In our approach, a constant DC voltage is supplied continuously to all nodes.

In this work we envision MLI as a fabric but conduct communication and power transfer by isolating a portion of the MLI ground layer and therefore mitigate the problem of high capacitance between the conductive layers of MLI. Also, since MLI layers are connected to ground by default, our approach maintains the main functionality of MLI.

3 Foundations for Considering MLI as Medium for Sensor Node Communication

In order to investigate the potential of using MLI as a communication medium, it is necessary to know its current carrying capacity, i.e., to make sure that the heat generated as a result of current flow through the MLI will not burn it. We calculate the resistance for the MLIs with different coatings: aluminum, silver and gold. The values for the coating thickness are from the literature [1].

The thickness of the aluminum, silver and gold coatings are $0.1 \mu\text{m}$, $0.15 \mu\text{m}$ and $0.09 \mu\text{m}$ respectively [1]. We calculate the resistance of the above mentioned MLIs using Eq. 1. It is necessary to note that this formula is applicable in our case since the geometry of the MLI is a straight sheet [1]:

$$R = \rho \frac{L}{A} \quad (1)$$

where ρ , L and A are the MLI resistivity, length and cross-sectional area respectively. Table 1 illustrates the resistance values of the MLIs with the coatings mentioned above. We assume a current consumption of 10 mA for a sensor node (i.e., a sensing circuit and a microcontroller) given the increasing rate in power reduction of microcontrollers and sensing circuits [15]. Taking into account the values from Table 1 and the 10 mA current, the heat generated over the MLI with a current of 10 mA is on the order of μJ as illustrated in Fig. 2. This amount of heat is low and does not

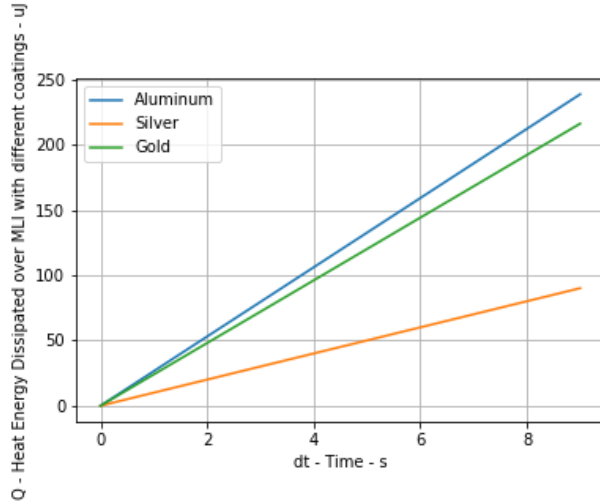


Figure 2. Heat generated across the 0.5x0.5m MLIs with aluminum, silver and gold coatings and 10 mA current.

Table 1. MLI Resistance with Different Coatings

Coating	Resistivity @ 20°C (Ωm)	Length (m)	Area (m^2)	R (Ω)
Aluminum	$2.65 \cdot 10^{-8}$	0.5	$5 \cdot 10^{-8}$	0.265
Silver	$1.6 \cdot 10^{-8}$	0.5	$7.5 \cdot 10^{-8}$	0.1
Gold	$0.022 \cdot 10^{-6}$	0.5	$4.5 \cdot 10^{-8}$	0.24

generate excess heat or degrade the MLI functionality.

If we assume that 10 sensor nodes are embedded in an MLI, then the MLI needs to withstand currents on the order of 100 mA. Therefore, we carry out an experiment at room temperature to determine the MLI current carrying capacity. Fig. 3 illustrates the experiment setup. We conduct the experiment with an MLI having Vacuum Deposited Aluminum (VDA) on both sides and Mylar as its substrate. The MLI was provided by the European Space Agency (ESA).

We set the power supply to 5 V and increase the current step-wise from 1 mA to 160 mA. We use a thermocouple to measure the MLI temperature. The experiment shows that the temperature difference across the MLI and the air is almost 2°C. The results from this experiment indicate that the MLI can withstand currents on the order of 100 mA at room temperature, i.e., assuming a sensor node consumes 10 mA, then with 10 sensor nodes there will still be no excessive heating across the MLI at room temperature.

4 MLI Communication Platform

Based on the results from the experiment in the previous section, we develop a schematic solution in order to demonstrate the feasibility of communication between transmitters across the MLI. Two layers of MLI and the spacer between them (Fig. 1) form a capacitive layer. Therefore, the transmission line has a capacitive behavior. Compared to Noda et al.'s work [12] where two carrier frequencies were used (one for clock and the other for data) due to the use of I2C

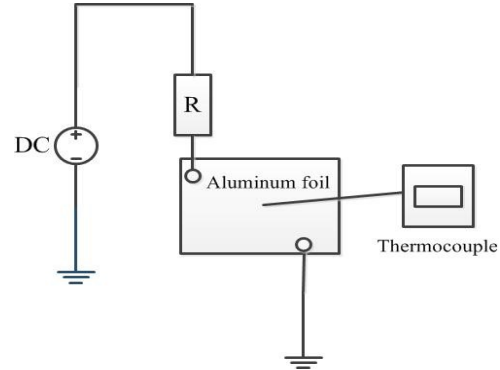


Figure 3. Experiment setup for determining the current carrying capacity of MLI.

interfaced sensors, in this work we do not use an I2C and we employ Manchester coding for data transmission and therefore the signal is self-clocked. In terms of miniaturization of sensor nodes embedded in MLI, our approach could be deemed practical since we decrease the number of interconnections in a circuit, i.e., eliminate the clock line and therefore we can choose components with a lower number of pins. Also, the use of Manchester coding provides a robust way for extracting the DC component of the data signal. We set the frequency of the carrier signal to 1.59 MHz and modulate it using amplitude-shift keying (ASK) by transmitting or grounding the carrier signal. 1.59 MHz was chosen arbitrarily as the purpose of this work is to demonstrate the feasibility of communication and power transfer through MLI. The chip rate is 1kHz. Fig. 4 illustrates the block diagram of the platform. The figure shows that the platform consists of the following parts: 1. Carrier signal generation 2. Data generation 3. Switch 4. Bandpass filter 5. AC coupling 6. Detector 7. Demodulator and 8. a microcontroller unit (MCU). The transmission medium acts as a capacitor connected in parallel to the switch in Fig. 4. For periods when the switch is open (the carrier signal is not grounded, i.e., when it is transmitted to the receiver node), the higher the capacitance of the transmission line, the more signal attenuation occurs.

We perform a separate experiment to determine the effect of capacitance on signal amplitude. In this experiment, we connect two transmitters to each other directly and test the communication between them. We observe the carrier signal and the demodulator output on the receiver (Figures 6 and 5). Then we start adding capacitors between the transmitter and the receiver, i.e., we simulate a capacitive transmission line. We increase the capacitance from 100 pF to 700 pF and observe the carrier signal and the demodulator output for each capacitance value. We do not observe high signal attenuation in this range and the signal has almost the same level as the case when the two transmitters are connected

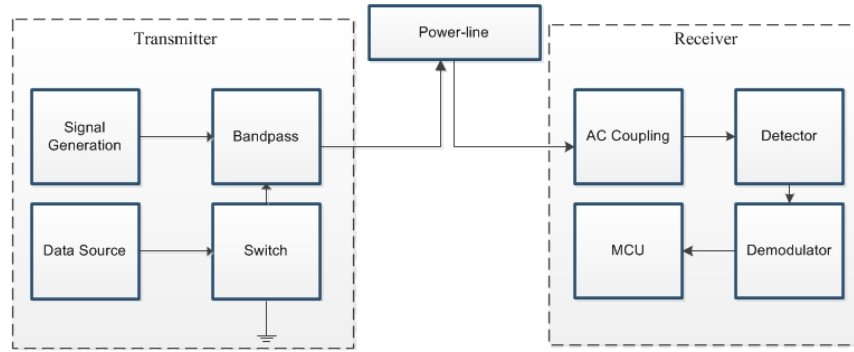


Figure 4. Block diagram of our MLI communication platform

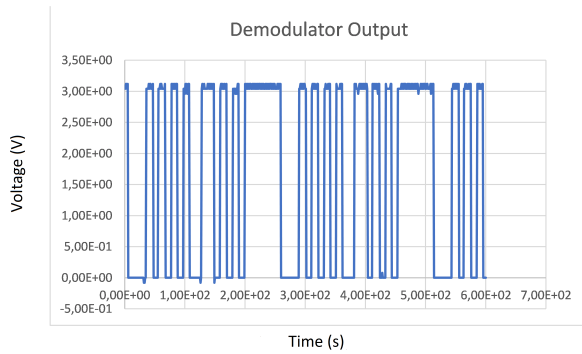


Figure 5. Demodulator output @ both 100pF & 700 pF

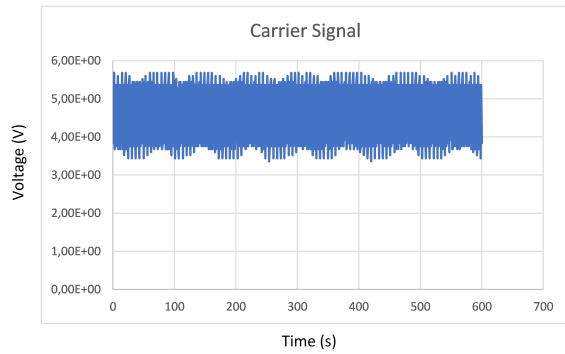


Figure 6. Capacitance effect on carrier signal @ both 100 pF & 700 pF

to each other without capacitors in between, i.e., Fig. 5 and Fig. 6. Therefore, if an MLI has a capacitance in the 100-700 pF range and we use our developed communication platform with a 1.59 MHz carrier signal, we expect to have low attenuation.

5 Evaluation of MLI Communication Platform

In this section, we demonstrate experiments in which we use our communication platform to investigate the feasibility of using MLI as communication medium.

Motivation. Based on the obtained results from theoretical calculations of the dissipated heat, small temperature differ-

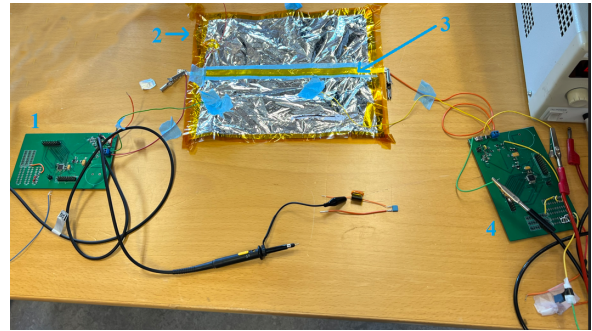


Figure 7. Experiment setup for determining the feasibility of communication over MLI: 1. Transmitter 2. MLI 3. Transmission line 4. Receiver

ence between the MLI and the ambient air, and the signal transmission experiment in the 100-700 pF range, we investigate the feasibility of communication between two transmitters through MLI.

Setup. The setup is demonstrated in Fig. 7. We use a 5V supply voltage. The frequency of the carrier signal and the duration of each logic level (chip) are 1.59 MHz and 1 ms respectively. The capacitance of the MLI is 212 nF. The size of the MLI is 30x20cm.

Results and Analysis. First we assign one MLI layer as power and the other as ground. Then we connect the transmitter and receiver to the MLI and apply 5 V to the transmitter. We observe that we receive 5 V at the receiver. The carrier signal, however, experiences a high attenuation which is due to the 212 nF capacitance of the MLI. At 212 nF, less reactance appears on the signal transmission path. In order to rectify this issue, we place an LC circuit parallel to the MLI and repeat the experiment. Given the fact that the MLI can be represented as a 212 nF capacitor, we need to place an inductor in parallel to the MLI. However, as the 5V is also transmitted with the signal, the inductor can provide a short path for the DC component of the signal. Therefore, we connect a 1nF capacitor in series with the inductor. Given the 1nF capacitance, the capacitance of MLI and the frequency of the carrier signal, the value of the inductor will be almost 10 uH. However, adding the LC parallel resonance did not mitigate the problem and we observe only 5 V at the receiver.

As a solution to this problem, we isolate a small portion of

the MLI, either by taping two lines on the ground plane and use the area between the two lines as a conductive medium or by adding a stripe line on top of the MLI surface and use that stripe line for communication. We use the latter and place a stripe line of a length of 30 cm and a width of 1 cm over the MLI. The strip line was made of aluminum, i.e., the same material as the MLI surface. We connect the transmitter to one end of the line and the receiver to the other end as shown in Fig. 7. We observe the modulated carrier signal along with the DC component which is similar to Fig. 6.

Our results demonstrate that it is possible to isolate a portion of the MLI and use it as a transmission line. Using this configuration, we have avoided the problem with the high capacitance between the MLI layers. Since the MLI conductive layers are grounded by default and we use a dedicated area on the MLI surface for signal transmission, we do not change the functionality of the MLI (compared to the case when one assigns one MLI layer as power and the other as ground). This means our proposed method is non-intrusive. Since the transmission line carries both signal and power, we can use it as a shared bus for power transfer and communication when connecting multiple sensor nodes to it.

6 Conclusions

In this work, we investigate the feasibility of using MLI as medium for signal and power transmission. First, we provide theoretical and experimental rationales of why we consider MLI as a transmission medium. Then, we present a schematic solution for communication over MLI. Our experimental results indicate that if we assign one layer of MLI as power and the other as ground and transmit data over the power layer, then the high capacitance of MLI attenuates the signal drastically. However, if we isolate a portion of the MLI surface for signal and power transmission and the other portion of the same surface as ground, we avoid the problem of the high capacitance between the MLI layers and enable power and data transmission over MLI. Moreover, this approach is non-intrusive in the sense that we do not change the default configuration of the MLI layers compared to the case where one assigns one layer for power and signal transmission and the other as ground. We propose MLI as a shared bus through which sensor nodes can communicate and transfer power.

Acknowledgement

This work has been financially supported by the Swedish Foundation for Strategic Research. We also acknowledge the kind support by Mr. Romain Peyrou-Luaga, at the Thermal Division of ESA ESTEC, Netherlands, for providing the thermal blanket (MLI) used in the experiments.

7 References

- [1] *Sheldahl: The Red Book*, Sheldahl, Inc. 2020.
- [2] A. Baranov, D. Spirjakin, S. Akbari, A. Somov, and R. Passerone. Poco: ‘perpetual’ operation of co wireless sensor node with hybrid power supply. *Sensors and Actuators A: Physical*, 238:112–121, 2016.
- [3] G. C. Birur, G. Siebes, and T. D. Swanson. Spacecraft thermal control. In R. A. Meyers, editor, *Encyclopedia of Physical Science and Technology (Third Edition)*, pages 485–505. Academic Press, New York, third edition edition, 2003.
- [4] J. M. Corchado, J. Bajo, D. I. Tapia, and A. Abraham. Using heterogeneous wireless sensor networks in a telemonitoring system for health-

- care. *IEEE Transactions on Information Technology in Biomedicine*, 14(2):234–240, 2010.
- [5] K. K. de Groh, B. A. Banks, S. K. Miller, and J. A. Dever. Chapter 28 - degradation of spacecraft materials. In M. Kutz, editor, *Handbook of Environmental Degradation of Materials (Third Edition)*, pages 601–645. William Andrew Publishing, third edition edition, 2018.
- [6] D. Dooling. *Multilayer Insulation Guidelines*. National Aeronautics and Space Administration - NASA.
- [7] C. Durin, J. Mandeville, and J. Perrin. Active detection of micrometeoroids and space debris sodad-2 experiment on sac-d satellite. *Advances in Space Research*, 69(10):3856–3863, 2022.
- [8] R. Funase, S. Ikari, K. Miyoshi, Y. Kawabata, S. Nakajima, S. Nomura, N. Funabiki, A. Ishikawa, K. Kakihara, S. Matsushita, R. Takahashi, K. Yanagida, D. Mori, Y. Murata, T. Shibukawa, R. Suzumoto, M. Fujiwara, K. Tomita, H. Aohama, K. Iiyama, S. Ishiwata, H. Kondo, W. Mikuriya, H. Seki, H. Koizumi, J. Asakawa, K. Nishii, A. Hattori, Y. Saito, K. Kikuchi, Y. Kobayashi, A. Tomiki, W. Torii, T. Ito, S. Campagnola, N. Ozaki, N. Baresi, I. Yoshikawa, K. Yoshioka, M. Kuwabara, R. Hikida, S. Arao, S. Abe, M. Yanagisawa, R. Fuse, Y. Masuda, H. Yano, T. Hirai, K. Arai, R. Jitsukawa, E. Ishioka, H. Nakano, T. Ikenaga, and T. Hashimoto. Mission to earth–moon lagrange point by a 6u cubesat: Equuleus. *IEEE Aerospace and Electronic Systems Magazine*, 35(3):30–44, 2020.
- [9] X. Liu, Y. Hou, J. Liu, X. Yang, Y. Li, X. Xu, and X. Zhu. Design and implementation of distributed temperature monitoring system based on fiber optic temperature sensor. In *2019 4th International Conference on Mechanical, Control and Computer Engineering (ICMCCE)*, pages 150–1503, 2019.
- [10] S. Narayana, R. V. Prasad, V. S. Rao, and C. Verhoeven. Swans: Sensor wireless actuator network in space. In *Proceedings of the 15th ACM Conference on Embedded Network Sensor Systems*, pages 1–6, 2017.
- [11] A. Noda and H. Shinoda. Frequency-division-multiplexed signal and power transfer for wearable devices networked via conductive embroideries on a cloth. In *2017 IEEE MTT-S International Microwave Symposium (IMS)*, pages 537–540, 2017.
- [12] A. Noda and H. Shinoda. Inter-ic for wearables (i 2 we): Power and data transfer over double-sided conductive textile. *IEEE transactions on biomedical circuits and systems*, 13(1):80–90, 2018.
- [13] A. B. Noel, A. Abdaoui, T. Elfouly, M. H. Ahmed, A. Badawy, and M. S. Shehata. Structural health monitoring using wireless sensor networks: A comprehensive survey. *IEEE Communications Surveys & Tutorials*, 19(3):1403–1423, 2017.
- [14] N. Pavlidou, A. H. Vinck, J. Yazdani, and B. Honary. Power line communications: state of the art and future trends. *IEEE Communications magazine*, 41(4):34–40, 2003.
- [15] STMicroelectronics. *Ultra-low-power 32-bit MCU Arm®-based Cortex®-M0+, up to 64KB Flash, 8KB SRAM, 2KB EEPROM, LCD, USB, ADC, DAC*.
- [16] M. Toda, J. Akita, S. Sakurazawa, K. Yanagihara, M. Kunita, and K. Iwata. Wearable biomedical monitoring system using textilenet. In *2006 10th IEEE International Symposium on Wearable Computers*, pages 119–120. IEEE, 2006.
- [17] E. Wade and H. Asada. Conductive fabric garment for a cable-free body area network. *IEEE Pervasive Computing*, 6(1):52–58, 2007.
- [18] A. A. Zhilenkov, D. D. Gilyazov, I. I. Matveev, and Y. V. Krishtal. Power line communication technologies in automated control systems. In *2017 IEEE Conference of Russian Young Researchers in Electrical and Electronic Engineering (EIconrus)*, pages 246–249, 2017.